Quaternary Research (2017), **87**, 407–422.

doi:10.1017/qua.2017.18

One thousand seven hundred years of interaction between glacial activity and flood frequency in proglacial Lake Muzelle (western French Alps)

Laurent Fouinat[a]*, Pierre Sabatier[a], Jérôme Poulenard[a], David Etienne[b], Christian Crouzet[c], Anne-Lise Develle[a], Elise Doyen[d], Emmanuel Malet[a], Jean-Louis Reyss[e], Clotilde Sagot[f], Richard Bonet[f], Fabien Arnaud[a]

[a]EDYTEM, Université Savoie Mont Blanc–CNRS, 73376 Le Bourget-du-Lac Cedex, France
[b]CARRTEL, Université Savoie Mont Blanc, 73376 Le Bourget-du-Lac, France
[c]ISTERRE, Université Savoie Mont Blanc–CNRS, 73376 Le Bourget-du-Lac, France
[d]INRAP, 51520 Saint-Martin sur-le-Pré, France
[e]LSCE, Université de Versailles Saint-Quentin CEA-CNRS, Avenue de la Terrasse, 91198 Gif-sur-Yvette Cedex, France
[f]Parc National des Ecrins, Domaine de Charance, 05000 Gap, France

(Received January 25, 2016; Accepted January 27, 2017)

Abstract

Local glacial fluctuations and flood occurrences were investigated in the sediment sequence of proglacial Lake Muzelle. Based on geochemical analysis and organic matter content established using loss on ignition and reflectance spectroscopy, we identified six periods of increased glacial activity over the last 1700 yr. Each is in accordance with records from reference glaciers in the Alps. A total of 255 graded layers were identified and interpreted as flood deposits. Most of these occurred during glacial advances such as the Little Ice Age period and exhibit thicker deposits characterized by an increase in the fine grain-size fraction. Fine sediment produced by glacial activity is transported to the proglacial lake during heavy rainfall events. The excess of glacial flour during these periods seems to increase the watershed's tendency to produce flood deposits in the lake sediment, suggesting a strong influence of the glacier on flood reconstruction records. Thus, both flood frequency and intensity, which is estimated based on layer thickness as a proxy, cannot be used in reconstruction of past extreme events because of their variability. There is a need to take into account changes in sediment supply in proglacial areas that could preclude satisfactory interpretation of floods in terms of past climate variability.

Keywords: Glacier fluctuations; Lake sediment; Flood reconstruction; French Alps

INTRODUCTION

Remote areas, such as high-altitude glacial environments, represent unique areas for detecting climatic changes and natural hazards following rapid changes (Gobiet et al., 2014). Two major concerns are related to glacier mass loss and precipitation regimes, which could influence modern ecosystems and civilization (Beniston, 2007). The recent behavior of Alpine glaciers presents clear evidence of atmospheric warming, which has resulted in a general decrease in glacier length in recent decades (Dyurgerov and Meier, 2000; Oerlemans, 2005; Diolaiuti et al., 2011). Glaciers are also known as very effective erosion agents, and the resulting sediment found in periglacial environments can be considered as a sensitive recorder of glaciological and climatic changes, given careful consideration of the glacial sedimentary system (Alley et al., 2003). A tendency for sediment yield to increase in larger glaciated basins was reported in Alaska by Hallet et al. (1996), as well as in the varved sediment of proglacial Lake Silvaplana in Switzerland (Leemann and Niessen, 1994). However, this is not always the case because the sediment export from glaciers also depends on subglacial shear and glaciofluvial processes operating near or directly beyond the glacial margin (Hodder et al., 2007). Glacial activity can transport supraglacial sediment, which is mostly composed of coarse sediment falling on the ice surface; on the other hand, sediment recovered from the subglacial area is composed of finer particles (Owen et al., 2003).

Detrital output from glaciers has, therefore, been extensively studied in proglacial lakes in order to reconstruct past glacier fluctuations over centennial to millennial time periods (Karlén, 1976; Nesje et al., 1991; Dahl and Nesje, 1994; Bakke et al., 2010; van der Bilt et al., 2015). Increased detrital input, as well as reduced organic matter abundance in

*Corresponding author at: EDYTEM, Université Savoie Mont Blanc–CNRS, 73376 Le Bourget-du-Lac Cedex, France. E-mail: Laurent.fouinat@univ-smb.fr (L. Fouinat).

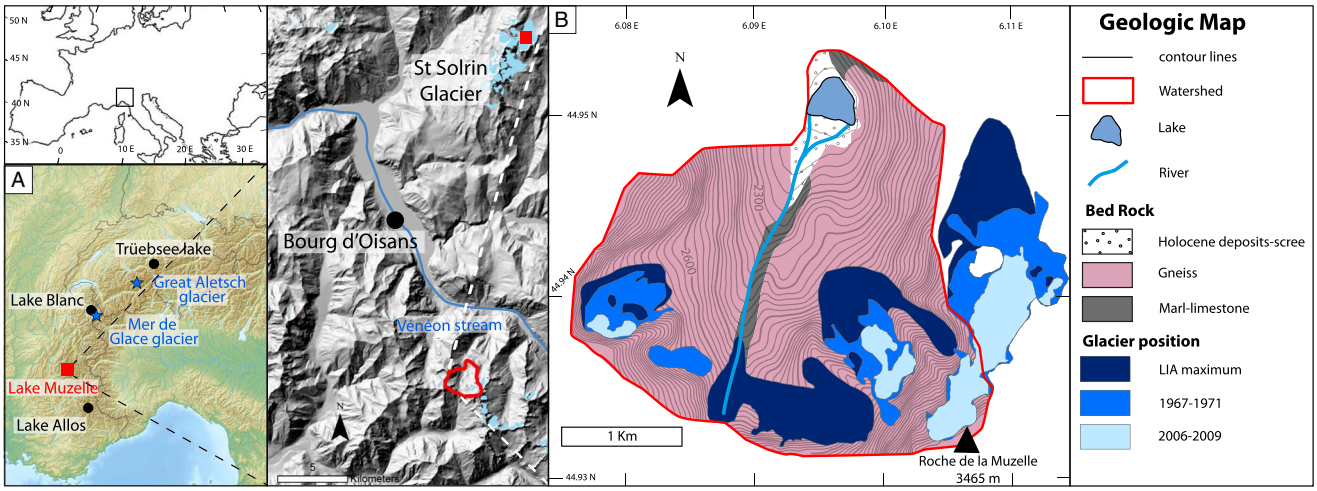

Figure 1. (color online) Geographic position of Lake Muzelle in the western Alps and locations of other records used in this study. Geologic map of the watershed with reported glacier positions from three different periods since the Little Ice Age (LIA; Gardent et al., 2014).

proglacial lakes, could be related to increased glacial activity, and these changes can be identified by reflectance spectroscopy (Rein and Sirocko, 2002; Rein et al., 2005; Debret et al., 2011; Trachsel et al., 2013). Fine sediments are then exported by subglacial streams to downslope areas and sometimes correspond to a majority of the sediment transported (Weirich, 1985; Hicks et al., 1990). In the context of glacial retreat, the sediment can be trapped temporarily in the watershed (Gilbert and Shaw, 1981; Navratil et al., 2012) or hydrologically disconnected from the stream (Micheletti and Lane, 2016), thus creating a temporal lag between sediment production and export in the watershed (Hodder et al., 2007). A major sediment transport mechanism in high-alpine watersheds is extreme rainfall events that trigger torrential floods, which are identified in high-altitude Alpine lakes as high-energy depositional layers (Arnaud et al., 2002; Giguet-Covex et al., 2012; Wilhelm et al., 2012, 2013, 2015, 2016; Wirth et al., 2013; Støren and Paasche, 2014). These extreme events essentially transport fine sediment (clay to sand) downstream; coarser sediment can be mobilized but contributes only a small proportion of the total sediment exported (Rickenmann et al., 1998). During a flood event, the presence of a large glaciated surface can promote faster runoff compared with a nonglaciated watershed, partly because of glacial meltwater, firn cover, or lower glacial snow thickness (Dahlke et al., 2012). Moreover, several studies on proglacial lakes have identified higher flood occurrence during periods favorable to glacier extension in the Alps (Glur et al., 2013; Swierczynski et al., 2013; Wirth et al., 2013; Amann et al., 2015). Those studies have highlighted the role of more frequent heavy rainfalls caused by changing atmospheric conditions, but there is a need for better understanding sediment availability linked to glacial variations on the reconstruction of the occurrence of flood events in high-alpine watersheds.

Here, we explored this relationship in proglacial Lake Muzelle, which is situated in the French Alps. The sediment record was investigated to reconstruct past glacial fluctuations and flood occurrences during the last 1700 yr. The record includes periods of warmer or drier climates, such as the Medieval Climate Anomaly (MCA) and the recent warming, and periods of colder or wetter climates, such as the Little Ice Age (LIA). The objective of this study was to reconstruct both the flood frequency and glacial fluctuations to explore the interaction between these two parameters based on sediment export through long-term variations of the hydrologic cycle.

Study area

Lake Muzelle (44°57.037′N, 6°5.845′E) is a proglacial lake located in the western Alps in France and lies at an altitude of 2100 meters above sea level (m asl). The lake has an area of 0.09 km^2, is 18 m deep and is ice-covered for 6 months of the year, from December to May. It is located approximately 30 km southeast of the city of Grenoble and is situated in a north-facing cirque. The 4.2 km^2 catchment area reaches a maximum elevation of 3465 m asl and includes a glacially covered area whose surface has drastically decreased over the last hundred years (Fig. 1). The maximum glacier extent was during the end of the LIA around AD 1850 (Gardent, 2014; Gardent et al., 2014). At its maximum LIA extent, the glacier occupied an area of ~1.1 km^2 (27% of the watershed). In the late 1960s, the glacier covered 0.5 km^2 (11% of the watershed), and in 2009, it covered approximately 0.2 km^2 (4.8% of the watershed). The Muzelle glacier is not entirely situated in the watershed of the lake, and only the upper part is now connected to the lake via a stream. The geologic setting is mainly composed of granite and gneiss, except for a small corridor underneath the permanent glacial stream composed of marls. The sediment supply to the lake consists mainly of bedrock material and poorly developed soils, and the sediment flows from the south to the lake, forming a large delta. No glacial moraine is present in the watershed. The site is

https://doi.org/10.1017/qua.2017.18 Published online by Cambridge University Press

currently used as a pasture area for sheep; it is an open environment mostly covered by alpine lawn close to the lake and bare rock in the upper watershed. This site is located in the restricted area of the Ecrins National Park, and a refuge was built next to the lake in AD 1968 to receive hikers during the summer season.

MATERIALS AND METHODS

In April 2012, cores were retrieved from the deepest part of Lake Muzelle (18 m depth; 44°57′02.0″N, 6°05′48.0″E) using a UWITECH piston corer with hammer action. The master core sequence (MUZ12) is composed of two coring holes. MUZ1201 was retrieved from the lake bottom with a 90-mm-diameter tube, and MUZ1202 was retrieved with a 63-mm tube. A short gravity core, MUZ12P5, was also taken to provide a well-preserved sample of the water–sediment interface. In June 2014, a set of nine short gravity cores (MUZ14P1 to MUZ14P9) distributed across the deep portion of the lake basin were retrieved using a UWITECH piston corer, allowing us to better understand sediment partitioning throughout the entire lake system. This method was used to increase the reliability of the flood intensity reconstructions (Jenny et al., 2014). All cores were split in half lengthwise and photographed at high resolution (20 pixels/mm). A detailed macroscopic description allowed us to determine the different sedimentary facies and to establish the stratigraphic correlations between cores. A composite core was built using clearly identifiable layers in the overlapping sections of cores MUZ1201 and MUZ1202 to obtain a 283.5-cm-long sediment sequence.

Loss on ignition

The loss-on-ignition (LOI) technique was used to estimate the fractions of organic matter and carbonate in the sediment following Heiri et al. (2001). In total, 216 samples were analyzed, based on the lithostratigraphy, with thicknesses ranging from 0.3 to 1.5 cm. Samples were taken from the sediment cores and dried (at 60°C) in a stove for 48 hours. They were then crushed and placed in an oven at 550°C for 4 hours to oxidize the organic matter (OM) fraction:

$$\% \text{ OM} \Leftrightarrow \text{LOI}_{550°C} = (\text{DW}_{60°C} - \text{DW}_{550°C}) / \text{DW}_{60°C} \times 100.$$

After determining the dry weight (DW) at 550°C, the samples were placed in a 950°C oven for 2 hours to oxidize the carbonate fraction:

$$\% \text{CaCO}_3 \Leftrightarrow \text{LOI}_{950°C} = (\text{DW}_{550°C} - \text{DW}_{950°C}) / \text{DW}_{550°C} \times 100.$$

The noncarbonate ignition residue (NCIR) was obtained by subtracting the $\text{LOI}_{550°C}$ and $\text{LOI}_{950°C}$ from the initial weight $\text{DW}_{60°C}$.

Reflectance spectroscopy

Reflectance spectroscopy was performed using a continuous step of 0.5 cm and a Konica Minolta CM-2600d spectrophotometer. Measurements were taken at 10 nm increments over the range of 360 to 740 nm. The analysis was performed on the oxidized sediment surface using a polyethylene film. We used a transparent polyethylene film to avoid bias in the measurement (Debret et al., 2006). We also used the specular component excluded–Commission Internationale de l'Eclairage L*a*b* mode (Minolta CM-2002) to eliminate any bias because of specular reflection. Analyses were carried out using a D65 illuminant (Minolta CM-2002), which corresponds to average daylight and has a color temperature of 6504 K and an aperture of 5 mm (Debret et al., 2006). Calibration based on $BaSO_4$ from an international standard was performed before each section. L*, an indicator of brightness, was used to identify different lithostratigraphic units. The relative absorption band depth (RABD) was then calculated between 660 and 670 nm (Wolfe et al., 2006; Boldt et al., 2015) to evaluate the total sedimentary chlorophyll and its diagenetic products, which have absorption maxima between 660 and 690 nm. We normalized the RABD by the mean reflectance; because water content is greater at the top of the core, its effect is to reduce the overall reflectance (Balsam et al., 1998) of sediment assessed using the RABD (I-band) (Rein and Sirocko, 2002).

$$\text{RABD}_{660;670} = \left\{ [(6^{*}\text{R}_{590} + 7^{*}\text{R}_{730})]13 / \text{R}_{\text{min}(660;670)} \right\}$$

$$\text{RABD (I-band)} = \text{RABD}_{660;670} / \text{R}_{\text{mean}},$$

where R_{590} = reflectance at 590 nm, R_{730} = reflectance at 730 nm, $R_{\text{min}(660;670)}$ = minimum reflectance at 660 or 670 nm, and R_{mean} = the mean reflectance of the sediment.

Grain-size measurements

Grain-size measurements were carried out on the composite core using a Malvern Mastersizer 800 particle sizer at a lithology-dependent sampling interval. Ultrasonication was used to dissociate particles and to avoid flocculation. Interbedded deposits were characterized on the basis of their median (D_{50}) and coarse (D_{90}–D_{99}) fractions (Passega, 1964). We also documented the thickness and $D_{90\text{max}}$ of each interbedded deposit.

Geochemistry

Geochemical analysis was carried out using an Avaatech X-ray Fluorescence Core Scanner (EDYTEM [Environnement et Dynamique des Territoires de Montagne] Laboratory, CNRS – University Savoie Mont Blanc) at a resolution of 1 mm. The X-ray beam was generated with a rhodium anode and a 125 µm beryllium window, which allow a voltage range of 7 to 50 kV and a current range of 0 to 2 mA. We used thin Ultralene film (4 µm) to avoid contamination of the measurement prism and desiccation of the sediment. The relative element intensities were expressed in counts per second (cps), and geochemical data were obtained with different settings according to the elements analyzed. Si, Al, K, Fe, Ti, and Ca were measured at 10 kV and 1 mA for 20 seconds, and Sr, Rb, Zr, Mn, Cu, Zn, Pb, and Br were

https://doi.org/10.1017/qua.2017.18 Published online by Cambridge University Press

Table 1. Radiocarbon ages for the Lake Muzelle sedimentary sequence. Bold samples correspond to excluded dates from age-depth modeling.

Sample name	Laboratory code	Depth (mm)	Sample type	^{14}C yr BP	AD range (cal yr)	Probability
MUZ12_01Aa	**Poz-59230**	**84.5**	**Roots and twigs**	**310 ± 35**	**1650–1483**	**95**
MUZ12-01A1b	SacA 32335	103	Plant macroremains	210 ± 30	1810–1728	48.5
MUZ12_01B1a	Poz-59232	106	Moss, herb remains	150 ± 35	1783–1717	29.9
MUZ12_01B1b	SacA38358	150	Plant macroremains	370 ± 30	1526–1448	54.7
MUZ12-02A2a	**SacA32337**	**166**	**Moss and roots**	**2545 ± 30**	**–740 to –799**	**49.2**
MUZ12_01B1c	Poz-59233	192.5	Wood remains	635 ± 30	1397–1339	55.5
MUZ12_01B2a	**Poz-59235**	**206.5**	**Moss and herb remains**	**1340 ± 30**	**714–645**	**83.6**
MUZ12_02A2b	Poz-59231	226.5	Roots and herb remains	1050 ± 40	917–1033	78.7
MUZ12-01B2a	**SacA 32336**	**235**	**Plant macroremains**	**1485 ± 30**	**645–536**	**94.3**
MUZ12_02A2c	SacA38359	247.5	Twig and herb remains	1275 ± 30	776–662	94.4

measured at 30 kV and 0.75 mA for 30 seconds. A principal component analysis (PCA) was performed on the geochemical and LOI results using R software, version 3.0.2 (R Development Core Team, 2011) to determine the statistical correlations between the results and the corresponding facies and to visualize the geochemical nature of the different units (Sabatier et al., 2010; Bajard et al., 2016).

Coprophilous fungal ascospore analysis

To examine the potential impact of animal grazing pressures on the reconstructed flood activity, *Sporormiella* accumulation rates were determined in sediment subsamples collected throughout core MUZ12. Erosion processes in high-elevation catchments may be modified by grazing activity through stamping soils (Giguet-Covex et al., 2012). The variability in grazing pressure in a catchment area can be reconstructed from the variations in the accumulation rate of coprophilous fungal ascospores of *Sporormiella* (HdV-113) (Etienne et al., 2013). During the sampling, event layers were avoided because they may correspond to high-turbidity conditions related to floods or mass-movement events that may have transported unusual quantities of *Sporormiella* ascospores or induced the remobilization of older sediments. Subsamples were chemically prepared according to the procedure of Faegri et al. (1989). *Lycopodium clavatum* tablets were added to each subsample (Stockmarr, 1971) to express the results in terms of accumulation rates (number/cm^2/yr). Coprophilous fungal ascospores were identified based on several reference catalogs (van Geel et al., 2003; van Geel and Aptroot, 2006) and counted following the procedure established by Etienne and Jouffroy-Bapicot (2014).

Chronology

The chronology of the Lake Muzelle sediment sequence is based on 10 ^{14}C measurements on terrestrial macroremains, short-lived radionuclide measurements, and paleomagnetic secular variations. The ^{14}C measurements were carried out using accelerator mass spectrometry (AMS) methods at the Poznan Radiocarbon Laboratory and at the Laboratoire de Mesure ^{14}C (LMC14) ARTEMIS at the CEA (Atomic Energy Commission) institute at Saclay (Table 1). The calibration curve IntCal13 (Reimer et al., 2013) was used for the ^{14}C age calibration. The short-lived radionuclides in the upper 30 cm of core MUZ12P5 were measured using high-efficiency, very low-background, well-type Ge detectors at the Modane Underground Laboratory (LSM) (Reyss et al., 1995). The measurement intervals followed the facies boundaries, resulting in an irregular sampling of approximately 1 cm. Five thicker beds (at depths of 3.5–4.2, 12.1–14.5, 22.8–23.9, 25.7–26.9, and 30.1–33 cm) were not analyzed because they were considered to be instantaneous deposits. Cesium-137 (^{137}Cs) and americium-241 (^{241}Am) were introduced into the environment at the end of the 1950s by atmospheric nuclear weapons tests, which peaked in AD 1963. The Chernobyl accident in AD 1986 also dispersed ^{137}Cs into the atmosphere of the Northern Hemisphere. Excess ^{210}Pb was calculated as the difference between total ^{210}Pb and ^{226}Ra activities. We then used the constant flux/constant sedimentation (CFCS) model and the decrease in excess ^{210}Pb to calculate the sedimentation rate (Goldberg, 1963). The uncertainties of the sedimentation rates obtained by this method were derived from the standard error of the linear regression of the CFCS model. Additional chronological markers were provided by paleomagnetic investigations. The magnetic measurements were carried out on U-channel subsampled cores using the three-axis 2-G Enterprises cryogenic magnetometer of the CEREGE laboratory (Aix-Marseille University). The natural remnant magnetization was progressively demagnetized using alternative field techniques with 10, 20, 30, 40, and 60 mT steps. Only one magnetic component is observed. PCA is performed using the PuffinPlot software package (Lurcock and Wilson, 2012) to calculate the characteristic remnant magnetization (ChRM). The ChRM direction (declination and inclination) versus depth was compared to known secular variations of the geomagnetic field to provide additional chronological markers. The geomagnetic field's secular variations are variable in space and time and have been measured in different laboratories since the seventeenth century. As MUZ is located between Paris, France (Alexandrescu et al., 1997), and Viterbo, Italy (Lanza et al., 2005), the ChRM curve is compared to both records.

https://doi.org/10.1017/qua.2017.18 Published online by Cambridge University Press

RESULTS

Core description and lithology

The sediment recovered from the 283.5-cm-long MUZ12 core is composed of homogenous clay to silt-sized mud intercalated with dark sandy layers. The homogeneous mud is characterized by three facies: f1 is a silty clay-rich, dark-brown-colored mud (2,5Y 4/2) with an average median grain size (D_{50}) of 24 µm; f2 is a clay-rich, brownish-gray-colored mud (2,5Y 5/2) with a slightly lower D_{50} of 19 µm (Fig. 2); f3 is an organic-rich (average of 5.3 wt%) mud layer that generally occurs in association with f1. These three facies are interbedded with layers of graded sand to silt corresponding to facies 4 (f4), which is almost always capped by a layer of clay-sized particles referred to as facies 5 (f5). Based on the identification of f1, f2, and f3, we separated the sediment cores into seven depositional units. Facies f1 and f3 are essentially present in unit 1 (0–35 cm), unit 3 (83.5–108 cm), unit 5 (150–190 cm), and unit 7 (216–283.5 cm), with mean LOI 550°C values of 4.4 wt% and high RABD (I-band) values related to their organic matter contents. In contrast, f2 is essentially present in unit 2 (35–83.5 cm), unit 4 (108–150 cm), and unit 6 (190–216 cm), with average LOI 550°C values of 3.6 wt% and low RABD (I-band) values. This sediment sequence leads to distinctive characterization of (1) a muddy facies (f1, f2, and f3) that corresponds to continuous sedimentation and (2) normally graded layers (f4 + f5) that are interpreted as instantaneous deposits (Fig. 2).

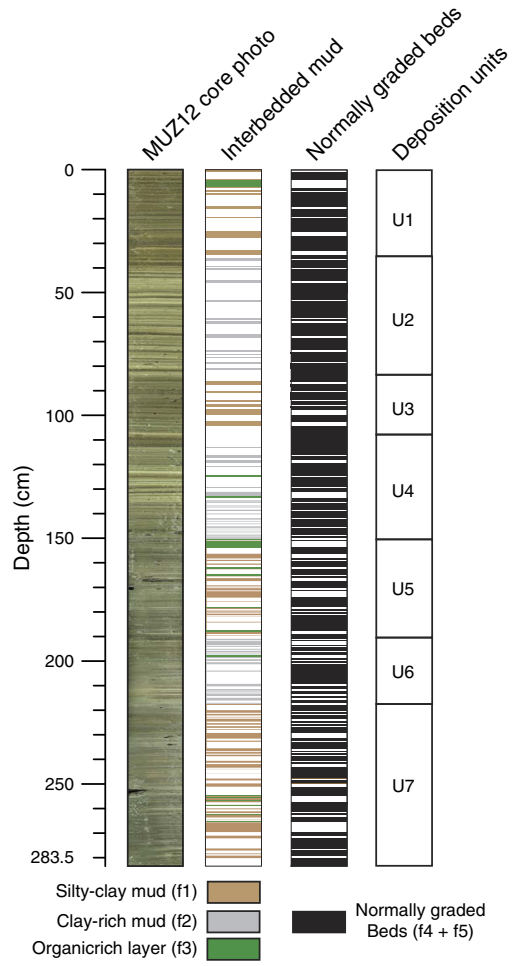

Figure 2. (color online) Photograph of the core and lithological description of the MUZ12 sediment sequence identifying interbedded clay mud and graded beds. The clay mud repartition is used to establish the depositional units.

Continuous sedimentation

Once facies f1, f2, and f3 were identified, we obtained a free-graded-bed accumulation of the 80.1 cm of clay mud (Fig. 3A). The correlation circle produced by PCA includes both geochemical and LOI results, highlighting the separation between the units (Fig. 3B). Dimensions 1 and 2 (denoted as Dim1 and Dim2) represent almost 59% of the total variability. On the left side (negative loading for Dim1), a first end member is characterized by RABD (I-band), LOI 550°C, and Br content that represents the organic-rich sediment within the core and makes up the main contribution to U1, U3, U5, and U7. On the right side (positive loading for Dim2), another end member could be defined based on the NCIR, Si, Al, Fe, and K contents. This end member represents the detrital part of the sediment and makes up the main contribution to U2, U4, and U6. The proportion of the mineralogical content of the sediment fluctuates from 89.8 wt% to 95.2 wt%, making it the dominant material in the sediment. The K and Ti contents are lower in f1; however, they are higher in f2, reaching the highest peaks in U2 and U4. Overall, organic matter varies in opposition to mineral content, demonstrating that units dominated by f2 (U2, U4, and U6) are periods of increased mineral deposition, which proportionally decreases the organic matter content in the sediment.

Normally graded beds

We investigated the spatial extent of all the normally graded beds (NGBs; f4 + f5) (Fig. 2) using the stratigraphic correlations between the nine cores taken in 2014 (Fig. 4). Based on the thickness of the graded beds from MUZ14P5 sediment core (center of the lake), we selected three clearly identified deposits (among the 15 correlated deposits) in all the cores. These deposits range in thickness from 2.7 cm (Fig. 4C) to 0.9 cm (Fig. 4B). These deposits were located on the bathymetric map in order to identify their spatial extents. For Figure 4B and C, the thicknesses of the deposits suggest that the sediment input originates from the eastern part of the delta (MUZ14P1) and then spreads to the central part, reaching a maximum sediment thickness in the central and northern parts of the lake. The most recent graded bed deposit (Fig. 4A) suggests that sediment input originates from the western part of the delta (MUZ14P3) and then spreads into the deeper part. The glacial stream and the delta are situated at the southern end of the lake, and the sediment is deposited in flood-related high-energy currents.

The graded layers (f4 + f5) are sometimes composed of terrestrial macroremains and present an erosive base related

https://doi.org/10.1017/qua.2017.18 Published online by Cambridge University Press

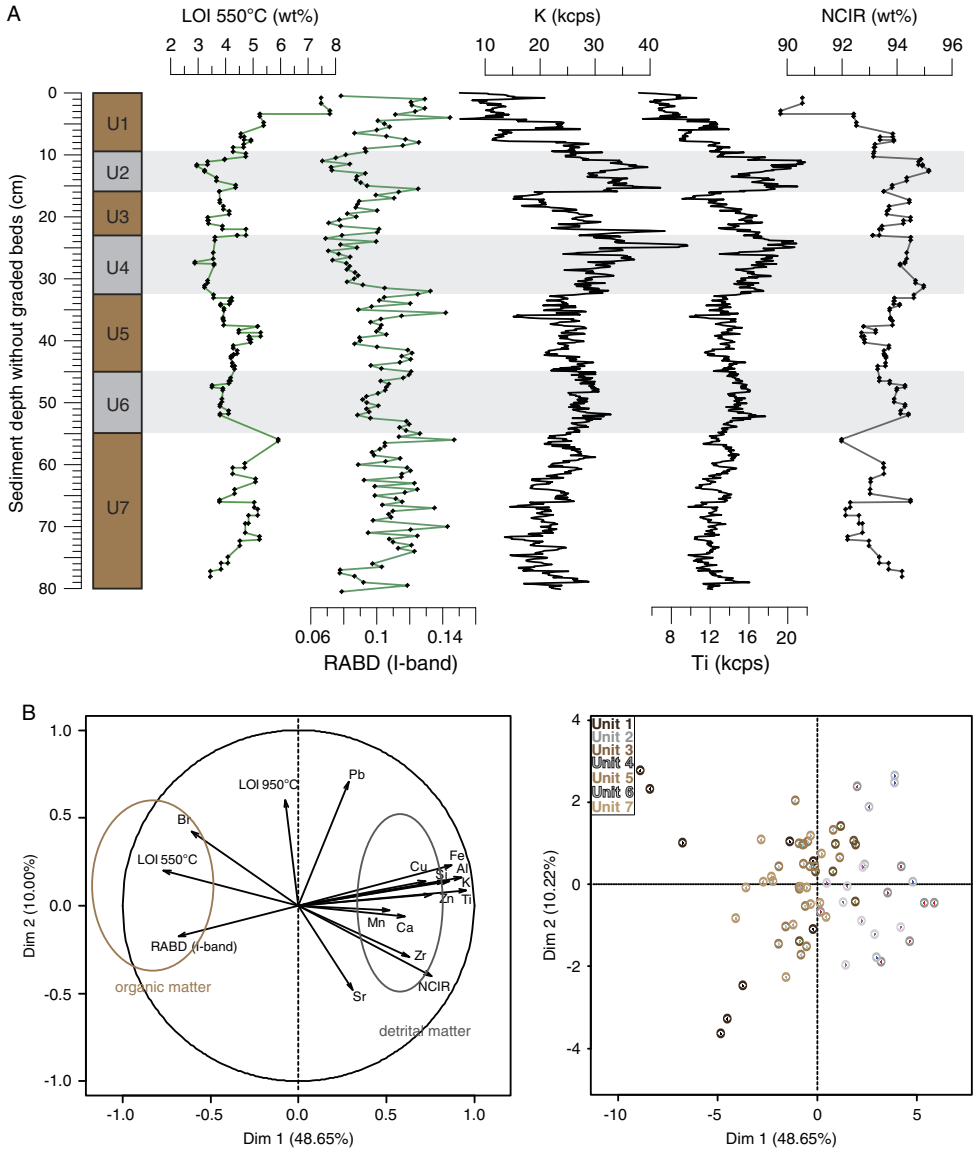

Figure 3. (color online) (A) Profiles of loss on ignition (LOI), relative absorption band depth (RABD; I-band), and geochemistry of the continuous sedimentation portion of MUZ12 core (not including the graded beds). NCIR, noncarbonate ignition residue. (B) Results of the corresponding principal component analysis based on the results of both geochemistry and LOI measurements and the associated population map.

to high-density currents triggered by flooding in the watershed. These deposits feature an average thickness of 0.8 cm, with a minimum of 0.1 cm and a maximum of 4 cm. Grain-size investigations allowed us to identify two types of NGBs with similar deposit thicknesses (Fig. 5A). We selected all 38 NGBs with thicknesses greater than or equal to 1.1 cm and explored their mean grain-size distribution (Fig. 5B). This allowed us to determine that NGB1 (black line) has a D_{50} value of 83 µm at its base and that the clay-sized cap has a D_{50} of 24 µm. In contrast, NGB2 has lower D_{50} values of 35 µm and 11 µm, respectively. Similarly, we investigated the D_{90max} and the thickness of these 38 NGBs, and we identified two linear relationships (Fig. 5C). The NGB1 (black diamonds) flood deposits have D_{90max} values ranging from 83 µm to 443 µm and thicknesses of 1.2 to 4 cm, with a well-constrained relationship between these two parameters ($n = 16$, $r = 0.96$, $P < 10^{-8}$). The NGB2 flood deposits (red dots) possess D_{90max} values of 49 to 116 µm and thicknesses of 1.3 to 3 cm, with a significantly different relationship ($n = 22$, $r = 0.84$, $P < 10^{-6}$). The results show lower D_{90max} values in NGB2; this could be related to proportionally fewer coarse grains or more fine sediment in this graded deposit type. To understand the differences between the NGB1 and NGB2 flood deposits, we plotted the f5 thickness (representing the finest fraction) against the total thickness of the deposit for the same 38 NGBs. In general, most of the NGB2 flood deposits possess thicker clay caps (f5), which leads to finer sediments than the NGB1 flood deposits. However, three of the NGB1 deposits feature thick clay caps, and two of the NGB2

https://doi.org/10.1017/qua.2017.18 Published online by Cambridge University Press

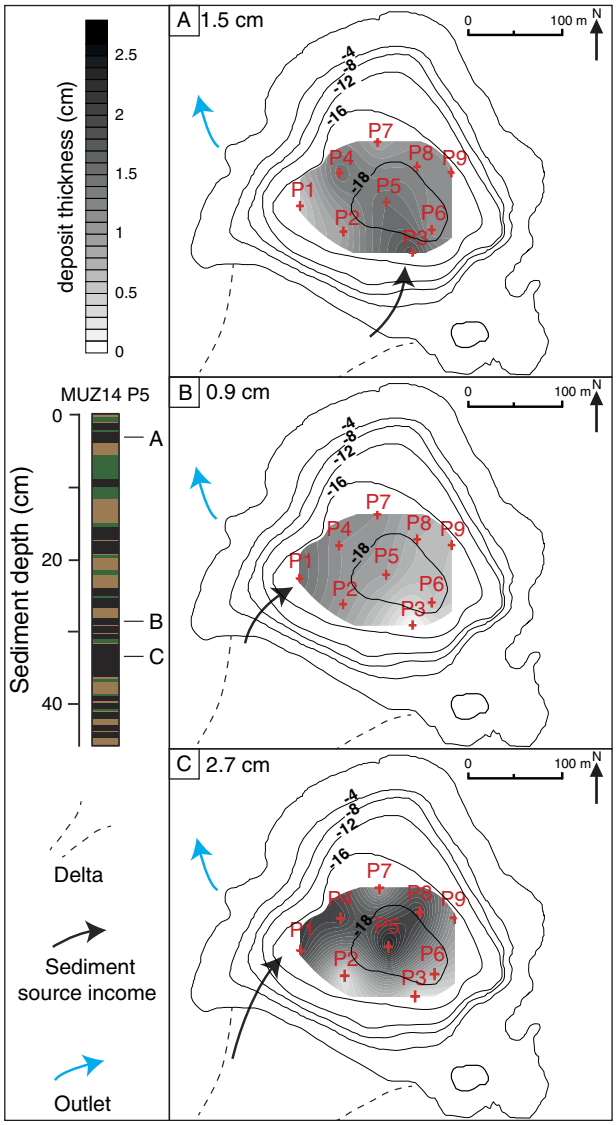

Figure 4. (color online) Spatial extent of three selected graded beds in the lake basin, as identified using nine correlated short gravity cores. Spatial extension of normally graded beds: (A) in AD 2006 (B) in AD1984 (C) in AD 1928.

deposits feature thin or absent f5 clay caps because of an overlying erosive deposit (indicated by the open red circle in Fig. 5C).

Chronology

The excess ^{210}Pb (^{210}Pb$_{ex}$) profile (Fig. 6) showed a regular decrease punctuated by drops in ^{210}Pb$_{ex}$ on the profile. Following Arnaud et al. (2002), these low values of ^{210}Pb$_{ex}$ correspond to NGBs and were excluded in order to construct a synthetic sedimentary record because they are considered to be instantaneous deposits. The ^{210}Pb$_{ex}$ activities plotted on a logarithmic scale revealed a linear trend (Wilhelm et al., 2012), which provided a mean accumulation rate (MAR) of 1.57 ± 0.4 mm/yr. Ages were then calculated using the CFCS model applied to the original sediment sequence to provide a continuous age-depth relationship. In addition, the profiles of ^{137}Cs and ^{241}Am present two (16.3 cm and 6.5 cm) and one (16.3 cm) peaks, respectively, corresponding to the high point of nuclear weapons testing in the Northern Hemisphere in 1963 for the lower peak and the Chernobyl accident in 1986 for the upper peak (Appleby et al., 1991). These two artificial peaks are in good agreement with the CFCS model (Fig. 6). In addition, we compared the historical flood calendar from the Vénéon River valley (Fig. 1) from the Restauration des Terrains en Montagne-Office Nationale des Forêts (RTM-ONF) database (http://rtm-onf.ifn.fr/) to the instantaneous deposits recovered in the lake sediment for the last 100 yr. Six flood events, occurring in 2006, 1984, 1947, 1928, 1922, and 1914, could be associated with the most significant NGB deposits, which occur at depths of 1–4.2, 7.1–8.6, 19.2–20.7, 23–26.5, and 30.1–32.9 cm. The good agreement between all these independent chronological markers and the ^{210}Pb$_{ex}$ ages strongly supports our age-depth model for the last century (Fig. 6).

Age-depth model based on 14C ages established by paleomagnetism

The ChRM declination profile of core MUZ1201B2 shows a change in the general trend at approximately 74 cm. Above this depth, the declination decreases; below this depth, it increases. This feature is clearly significant and is interpreted as corresponding to the D-1 change that occurred in AD 1820 ± 20 in Paris and in AD 1790 ± 20 in Viterbo (Fig. 7B). It is then possible to propose a coupled age/depth for this feature (AD 1810 ± 20 for 69–79 cm of depth) with good accuracy compared with the ^{14}C calibration curves, which have substantial error bars at this period (Fig. 7C). The ChRM inclination is noisy, which is likely because of the inhomogeneous grain size. Moreover, the Paris reference curve shows a change in the trend ca. AD 1700, whereas the one from Viterbo shows no change at this time. Therefore, we prefer not to use inclination as a chronological marker. The well-defined coupled age/depth values deduced from paleomagnetic investigations are combined with the short-lived radionuclide results and the ^{14}C ages to construct an age-depth model for the entire sediment core. Ten samples were dated to obtain ^{14}C ages (Table 1). Four were excluded because the ages were obviously too old, probably because of reworked material issuing from the watershed or contamination by macrophytes. To develop a well-constrained chronology, we removed the 255 graded beds interpreted as flood-induced deposits that represent 203 cm of instantaneous deposits. The remaining 80.5 cm (Fig. 7A) are used to construct a synthetic sedimentary record (Bøe et al., 2006; Giguet-Covex et al., 2012; Wilhelm et al., 2012). We then calculated an age-depth relationship via a smooth spline interpolation generated using R software and the R code package "Clam," version 2.2 (Blaauw, 2010). The age model is used to build the chronology of the flood deposits in Lake Muzelle during the last 1700 yr. Vertical bars represent the age of each flood thicker than 1 mm with the associated uncertainties (Fig. 7C).

https://doi.org/10.1017/qua.2017.18 Published online by Cambridge University Press

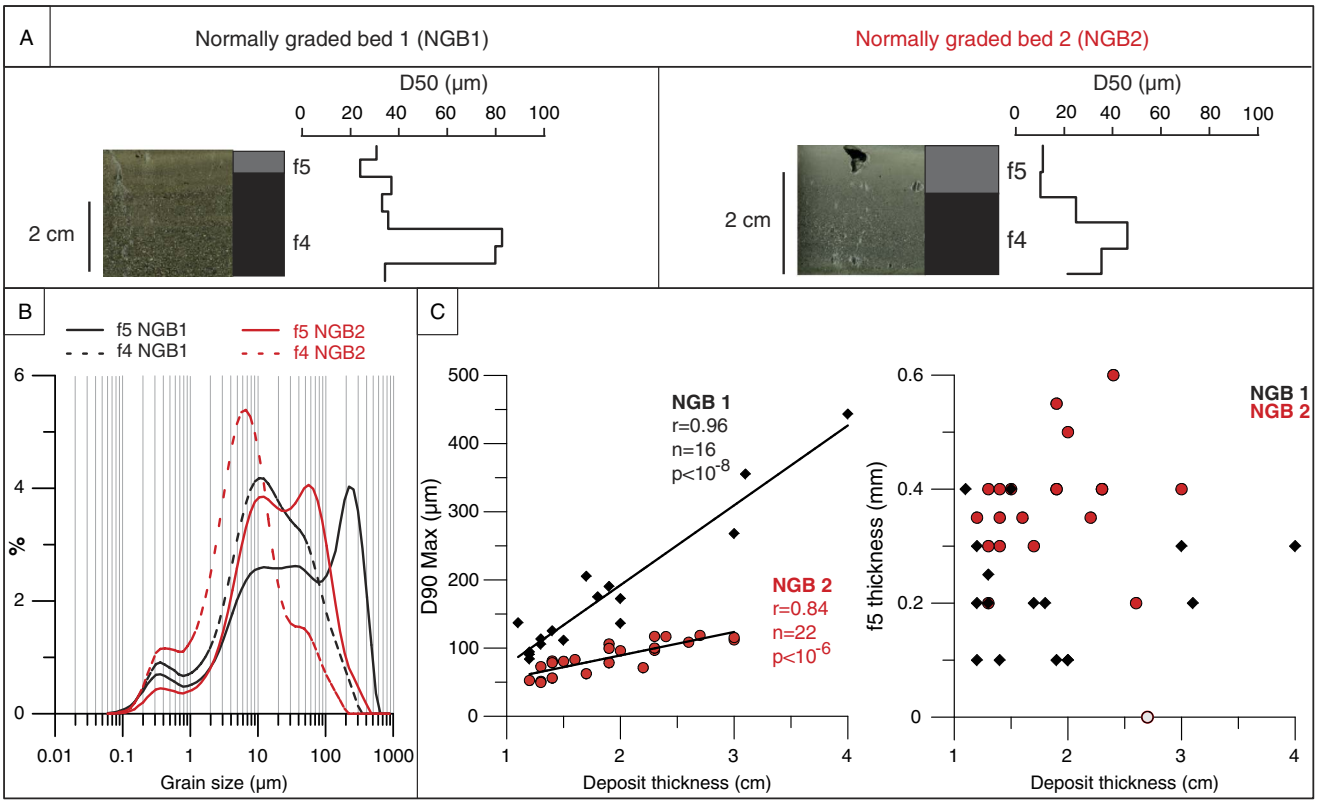

Figure 5. Grain-size distinctions between normally graded beds (NGBs) identified in the MUZ12 sediment core. (A) Photos and D_{50} (µm) for both NGB1 and NGB2. (B) Average grain-size distribution for facies 1 and facies 2. (C) Grain-size and thickness parameters of NGB1 and NGB2, which define two different linear trends between thickness and D_{90max}, and comparison of the thicknesses of the f5 facies and the main deposit from the same NGBs. The open red circle represents an NGB2 type flood without a clay cap. (For interpretation of the references to color in this figure legend, the reader is referred to the web version of this article.)

DISCUSSION

Past glacier fluctuations

The PCA results showed an anticorrelation between organic matter and detrital input in the Lake Muzelle sediments. The detrital end member (K and NCIR) corresponds to units U2, U4, and U6, which exhibited lighter sediment color (Fig. 3B). The proportion of organic matter in the sediment is less than 8 wt% but still allows differentiation of units U1, U3, U5, and U7 by their higher organic matter content and

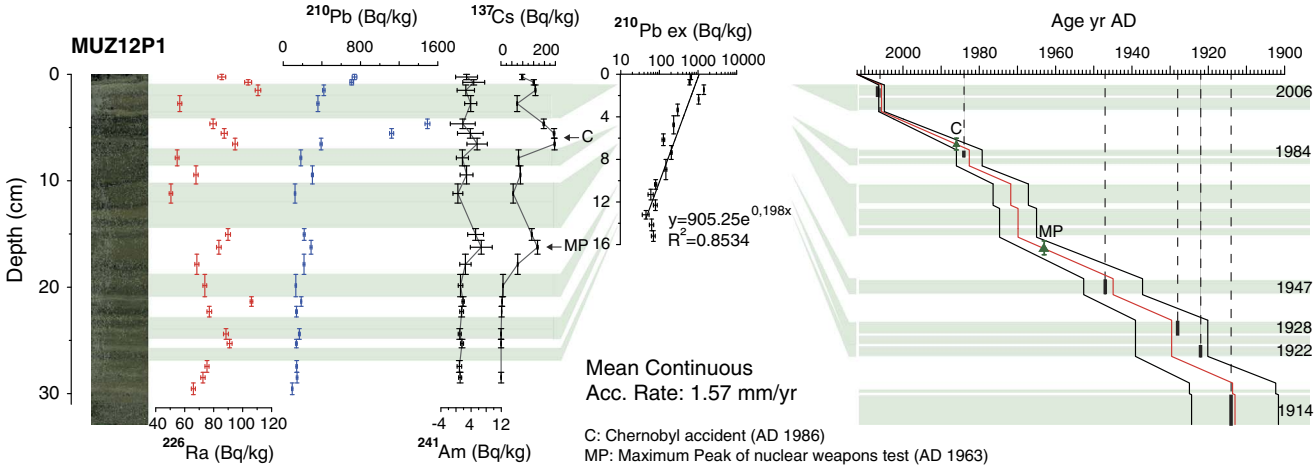

Figure 6. (color online) Profiles of ^{226}Ra, ^{210}Pb, ^{241}Am, and ^{137}Cs for core MUZ12P1 and application of a constant flux/constant sedimentation model to the synthetic sedimentary profile of excess ^{210}Pb (ignoring the normally graded beds [NGBs], which are considered to be instantaneous deposits). The resulting age-depth relationship, including 1σ uncertainties and indicating historical flood dates associated with NGBs, is also shown.

https://doi.org/10.1017/qua.2017.18 Published online by Cambridge University Press

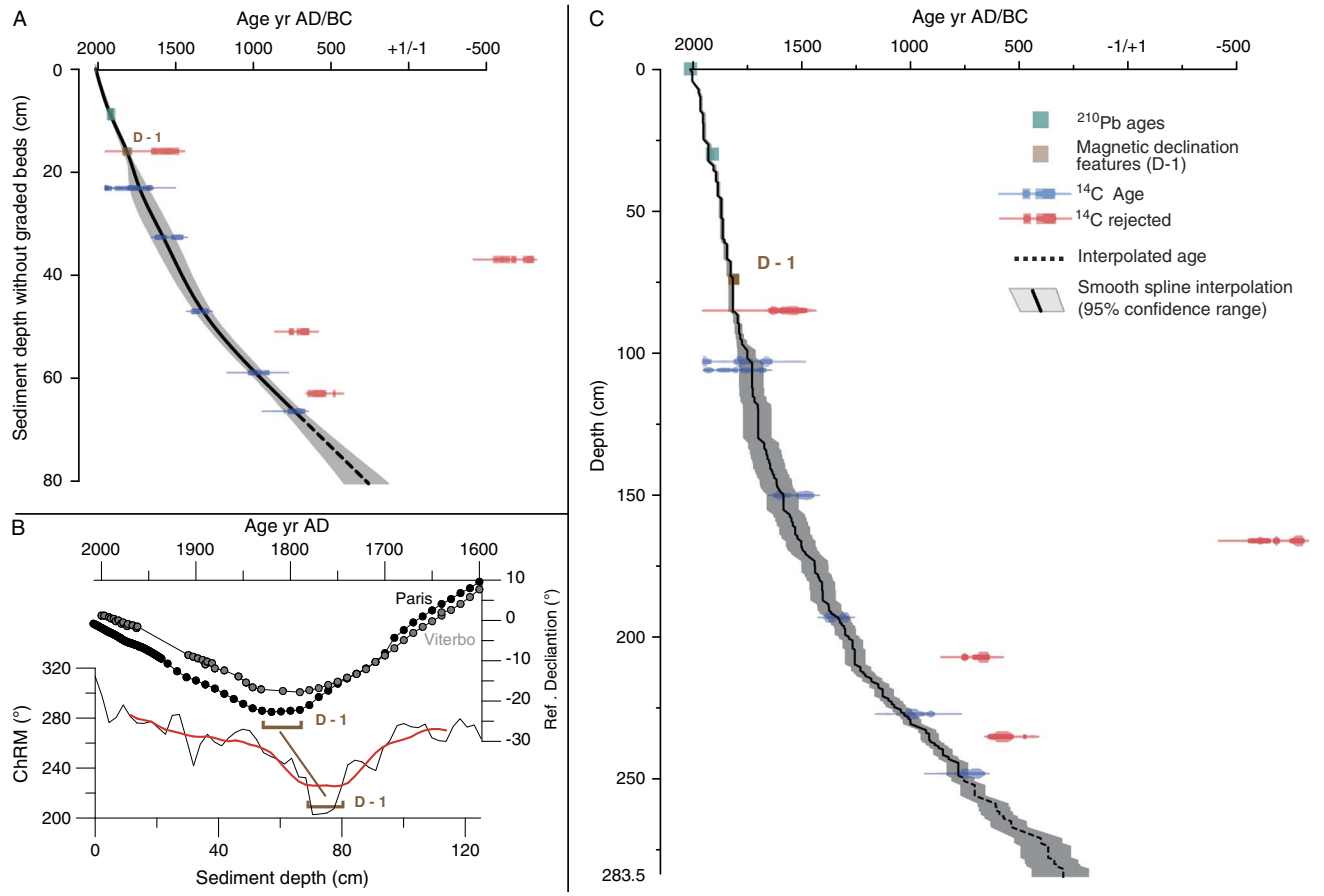

Figure 7. (A) Age-depth model for MUZ12 sediment sequence without normally graded beds (NGBs) produced with the "clam" R code package that combines historical ^{137}Cs peaks, ^{210}Pb-based sedimentation rates, ^{14}C ages, and magnetic declination features. (B) Correlative magnetic feature (D-1) between raw sediment characteristic remnant magnetization (ChRM; light gray), 20-cm running average (red curve), and variations in the geomagnetic declination in Paris and Viterbo (Alexandrescu et al., 1997; Lanza et al., 2005). (C) Age-depth profile for the entire MUZ12 sediment sequence, including NGBs marked by vertical sections, based on the results shown in panel A. (For interpretation of the references to color in this figure legend, the reader is referred to the web version of this article.)

darker sediment color. Nesje et al. (1991) used this differentiation to interpret high detrital input as glacier meltwater transport to proglacial lakes, whereas sediment rich in organic matter was deposited when glaciers were contracted or had melted away. Glaciers in the Alps produce fine sediment such as rock flour because of glacial abrasion (Owen et al., 2003), which is then transported further by glacial streams (Dahl et al., 2003). Consequently, several studies have observed higher sedimentation rates in proglacial lakes along with increased glacial cover (Hallet et al., 1996; Leonard, 1997; Menounos and Clague, 2008), but complex interactions between sediment availability and streams prevent consideration of the previous relationship as standard (Leonard, 1997; Hodder et al., 2007). If more erosion were to occur, more sediment would be transported to the lake, inducing higher detrital input that would dilute the organic matter produced in the lake (Nesje et al., 2001; Nussbaumer et al., 2011). In several proglacial environment studies, the organic matter variations were measured using reflectance spectroscopy analysis, allowing climate reconstructions (Debret et al., 2006; Trachsel et al., 2013; Boldt et al., 2015). Both of these parameters were investigated in Lake Muzelle and compared with other studies to test the representativeness of our sediment record.

The past 250 yr

Here, we provide a comparison between detrital input in the lake based on geochemical results (K) and organic matter content (inverted RABD [I-band]) since AD 1760. The two parameters were compared with glacial mass balance of St. Sorlin glacier (Fig. 8), which is located 10 km north of the study site and features an orientation and altitude comparable to the Muzelle glacier (Vincent et al., 2005). The main trend reflects decreases in both detrital input and St. Sorlin glacial mass balance during the observational period. The linear relationship between glacial mass balance and K is significant and positively correlated ($n = 65$, $r = 0.77$, $P < 10^{-13}$). The linear relationship between inverted RABD and glacial mass balance ($n = 26$, $r = 0.7$, $P < 10^{-4}$) is statistically significant. We interpret the lower detrital input in the lake as reflecting reduced glacial extent that decreased the amount of subglacial erosion

https://doi.org/10.1017/qua.2017.18 Published online by Cambridge University Press

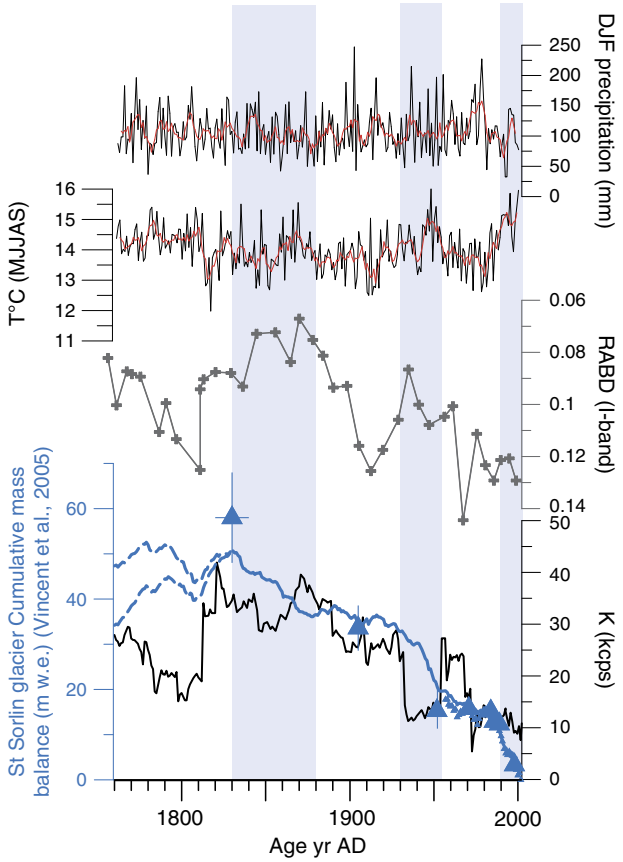

Figure 8. Comparison of Muzelle sediment potassium values measured by X-ray fluorescence (black line) and inverted relative absorption band depth (RABD; I-band) data with the cumulative mass balance of nearby St. Sorlin glacier during the past 250 yr (blue curve) based on direct measurements (small triangles), historical maps or photogrammetric measurements (large triangles), the reconstructed cumulative mass balance using a degree day model (plain blue line), and two models based on precipitation increases of 25% and 35% (dashed blue line) modified from (Vincent et al., 2005). Mean warm season temperature (°C) (May, June, July, August, and September [MJJAS]) and winter precipitation (December, January, and February [DJF]) using a 31-year running mean are also shown (Casty et al., 2005). (For interpretation of the references to color in this figure legend, the reader is referred to the web version of this article.)

and thus the detrital input (Leemann and Niessen, 1994; Ohlendorf et al., 1997; Koppes and Hallet, 2002).

In detail, there are three periods of rapid mass balance decrease (AD 1830–1880, AD 1930–1955, and AD 1990–2000) (blue bands in Fig. 8). These periods are characterized by higher summer temperatures (Casty et al., 2005) that probably contributed to the increased ablation of the St. Sorlin glacier (Vincent, 2002). During these periods of strongly negative glacial mass balance, the inverted RABD values are higher, denoting lower organic matter content in the sediment. However, K is recorded with a higher resolution, allowing the observation of low values at the beginning of the periods that suggest low detrital input in the lake. Similar features have been observed in the context of glacial retreat (Bogen, 1996; Hallet et al., 1996; Koppes and Hallet, 2002). At the end of each period, we observe a sharp increase in the K content (AD 1860–1880 and AD 1950–1970). More detrital input is thus transported into the lake. Between AD 1860 and 1880, higher K values occur at the same time as higher summer temperatures and relatively high autumnal precipitation values. The sharp increase in K content after AD 1950 occurs right after higher summer temperatures and during higher autumnal precipitations. The sediment input in the lake seems decoupled from the glacial extent at small scales. This temporal lag between sediment production by the glacier and glaciofluvial transport to the lake may be related to temporary sediment storage in the watershed (Gilbert and Shaw, 1981; Weirich, 1985; Desloges, 1994; Navratil et al., 2012). In a rapid glacial retreat context, Micheletti and Lane (2016) observed meltwater runoff increase at the expense of sediment export because of poor stream connectivity to recently deglaciated sediment storage zones. In this case, heavy rainfall could be favorable to sediment transport to the lake. As these sharp increases in K content occur after rapid glacial mass balance loss, the temporal lag at a seasonal scale can also be explained by pulses of sediment originating from glacial meltwater under constant runoff conditions and attributed to faster basal sliding (Riihimaki et al., 2005). Moreover, detrital inputs into the lake linked to glacial variations can be tracked by both K content and inverted RABD (I-band), but only for subcentennial variations. To better understand the complex detrital input variations at a decadal scale, further investigation into sediment transport to Lake Muzelle is necessary.

The last 1700 yr

We present the detrital input of Lake Muzelle based on K content (Fig. 9E) and inverted RABD (I-band) (Fig. 9D) values in the sediment during the last 1700 yr. Six periods of higher clastic sediment deposition were identified (AD 370–500,

Figure 9. The Muzelle sediment sequence record, which includes flood deposit thicknesses with associated flood types (A); the flood record, which is based on a 31-year running average (B); *Sporormiella* accumulation rates (number/cm^2/yr) indicating grazing activity in the surroundings of Lake Muzelle (C); inverted organic matter content in the sediment (relative absorption band depth [RABD]), which is used as a proxy of Muzelle glacial activity (D); and terrigenous input from Muzelle glacier (E). This record is compared to the Lake Allos flood calendar (F), which is shown using a 31-year running average, and records from reference glaciers, including mean accumulation rates (MARs) from Lake Trüebsee (G) (Glur et al., 2014), as well as frontal positions from the literature of the Great Aletsch Glacier (H) and Mer de Glace (I) (Holzhauser et al., 2005; Le Roy et al., 2015). (J) Central Europe summer tree ring-based temperature anomalies (June, July, and August [JJA]) (Büntgen et al., 2011) are also shown, using a 31-year running average. Blue bands indicate periods of greater glacial activity in Lake Muzelle. (For interpretation of the references to color in this figure legend, the reader is referred to the web version of this article.)

https://doi.org/10.1017/qua.2017.18 Published online by Cambridge University Press

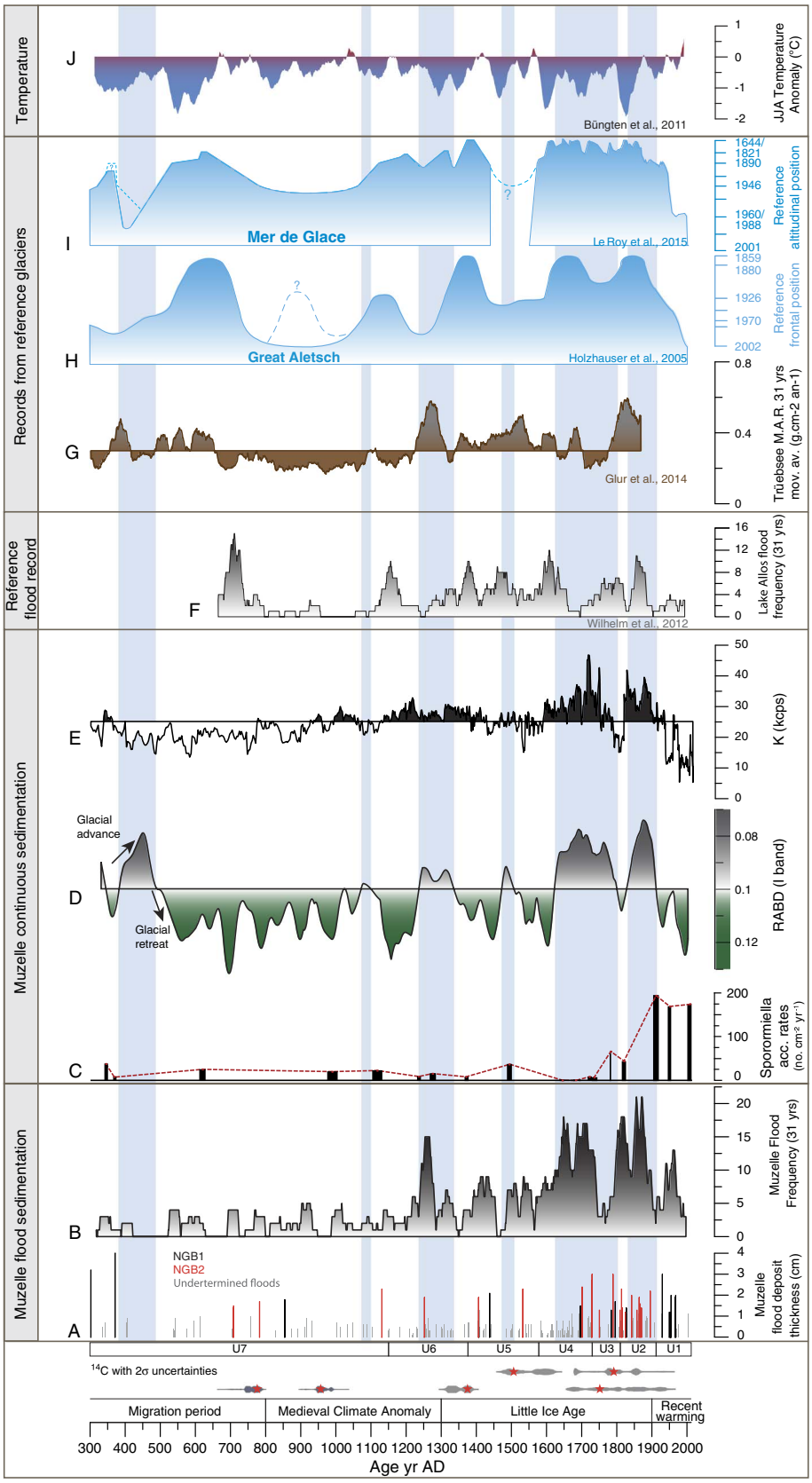

https://doi.org/10.1017/qua.2017.18 Published online by Cambridge University Press

AD 1080–1100, AD 1230–1325, AD 1460–1500, AD 1615–1790, and AD 1820–1900). The period of maximum detrital input occurred during the LIA, when the Muzelle glacier covered 27% of the watershed's area (Gardent et al., 2014). Comparison with records from both the Mer de Glace (Le Roy et al., 2015) and Great Aletsch (Holzhauser et al., 2005) reference glaciers shows that they exhibit similar trends. The reference glacier records show four major advances during the seventh, thirteenth, seventeenth, and nineteenth centuries and one minor advance during the twelfth century. Higher detrital input into Lake Muzelle occurred several decades before the Aletsch Glacier and the Mer de Glace increased in length, except during the LIA period, when they occurred at the same time. However, comparison with records reflecting fluctuations in smaller glaciers, such as proglacial Lake Trübsee (Glur et al., 2014) in the central Alps, shows that the period of higher detrital input into Lake Muzelle corresponds well with the increased MAR recorded in Lake Trübsee (Fig. 9G). The glacial advances during the fourth and thirteenth centuries, which were separated by several centuries of reduced glacier activity, are well recorded in both lakes. The detrital input of Lake Muzelle is also well correlated with the higher minerogenic content in Lake Blanc Huez, which is located 20 km to the north (Simonneau et al., 2014), highlighting the paleoclimatic response at the local scale. The three glacial advances recorded in Lake Trübsee during the LIA are also present in the Muzelle record, but the fifteenth-century advance lasted longer in the northern Alps, and the sixteenth-century glacial advance lasted longer in the western French Alps. The time lag between sediment production by glacier movement and the transport of sediment to the lake seems to be within ^{14}C age uncertainties in Lake Muzelle, suggesting limited temporary sediment storage in the watershed. Overall, the Lake Muzelle detrital input record is in accordance with records from Alpine reference glaciers. A better correspondence is obtained with small glaciers, probably because of their higher sensitivity to climatic parameters (Dyurgerov and Meier, 2000; Oerlemans and Reichert, 2000). Each of the periods of higher detrital input identified in Lake Muzelle occurred during a period of relatively low temperatures in central Europe (Büntgen et al., 2011). Thus, the Muzelle glacier seems to be sensitive to warm season temperatures, which is in accordance with several other alpine glaciers (Vincent, 2002; Vincent et al., 2005; Steiner et al., 2008).

Flood frequency

The flood record in Lake Muzelle, as reconstructed from the occurrence of graded beds, can be separated into two different phases. The first one, which lasted from AD 300 to AD 1300, exhibits very low flood frequency, with a maximum of 5 events occurring in 31 yr (Fig. 9B). The second one, which lasted from AD 1300 to the present, exhibits up to 20 events per 31 yr. Peaks of higher frequency are present when the detrital input is also higher, corresponding to glacial advances, especially at the end of the LIA. The synchronicity between flood deposition and higher glacial activity is remarkable; the question of interconnectivity of these two records is of particular interest.

The usual climatic forcing for flood deposition in high-altitude lakes is heavy precipitation during summer or autumn periods (Gilli et al., 2013; Wilhelm et al., 2013) when snow cover is minimal, whereas the classical climate forcings driving glacier changes are summer temperature (Glur et al., 2014; Le Roy et al., 2015) and winter precipitation (Holzhauser et al., 2005; Vincent et al., 2005), especially during the LIA period. In Lake Muzelle, flood occurrence is higher during periods of glacial advances, and flood deposit thickness is higher in the LIA. Flood characterization reveals two types of graded beds recorded in Lake Muzelle: NGB1, characterized by coarser grain sizes, and NGB2, characterized by finer grain sizes and a thicker clay cap facies (f5) (Fig. 5). Among the 38 NGB layers investigated using grain-size parameters, 60.5% were deposited during glacial advance, 87.5% of which were NGB2 (Fig. 9A). This feature has to be linked to a change in the watershed physical configuration that was either induced by human activities through pastoralism (Giguet-Covex et al., 2012) or by climate-induced change. As a test of this hypothesis, the counting of *Sporormiella* ascospores (Fig. 9C) in the continuously deposited sediment revealed a stronger influence of human practices no earlier than the eighteenth century and seems decoupled from the flood record in the Lake Muzelle watershed. The twentieth century is the period of maximum *Sporormiella* counts, as well as a period of decreasing flood frequency. Thus, human activities in the watershed do not seem to have any influence on flood deposition. However, increased glacier extent produces fine-grained sediment, such as rock flour, that is distributed in the terrigenous input and in the flood deposits. For the same thickness, the NBG2 flood deposits have a finer grain size compared with the NGB1 flood deposits, so there is an excess of fine sediment transported to the lake during periods of increased glacial extent. Thus, the thickness of flood deposits, which is used as an intensity proxy in other high-altitude systems (Bussmann and Anselmetti, 2010; Schiefer et al., 2011; Wilhelm et al., 2015), cannot be used in Lake Muzelle. Rather, it represents sediment availability in the watershed, linked to glacial fine-sediment production. Moreover, comparison of the Muzelle flood record with other flood records such as that from Lake Allos (Fig. 9F), which is located in the French Alps, shows major discrepancies during the MCA and LIA periods. Several high frequency peaks were identified during the MCA (Giguet-Covex et al., 2012; Wilhelm et al., 2012, 2013), which is the opposite of the Lake Muzelle record. During the LIA, the seventeenth century was a period of low flood frequency in both the northern and southern French Alps (Wilhelm et al., 2012, 2013), as well as in the central Swiss Alps (Glur et al., 2013). In contrast, the Lake Muzelle flood frequency record exhibits very high values at this period. The influence of large-scale atmospheric circulation during cold periods (Glur et al., 2013) does not seem to be the main driver of flood occurrence in the present study.

https://doi.org/10.1017/qua.2017.18 Published online by Cambridge University Press

The presence of the Muzelle glacier may have maintained favorable hydrologic conditions because of basal flow supplied by glacial meltwater, and the increased presence of fine sediment may have changed the sensitivity of the watershed to less intense rainfall events in summer or autumn at times of minimum snow cover. This mechanism could also perturb the flood frequency reconstruction in Lake Muzelle, and it is probably why the entire flood chronicle is not consistent with previous published studies from this area. The small glaciated watershed containing Lake Blanc (Wilhelm et al., 2013) does not appear to have the same influence on the flood frequency record as in Lake Muzelle. This may be because of the limited glacial surface extent or properties of the glacial geomorphology (e.g., moraines may interfere with sediment transport to the lake). Thus, glacial influence on flood chronologies seems to be site dependent and has to be checked in each studied system prior to interpreting flood reconstructions in terms of past climate variability. In the end, we interpret the presence of increased sediment availability during periods of increased glacier extent in Lake Muzelle as a major factor influencing the flood intensity proxy, as well as flood occurrence, through a change in watershed sensitivity to initiate flood deposits in the lake. This mechanism could be coupled with increased runoff caused by larger firn cover or glacial meltwater (Dahlke et al., 2012).

CONCLUSIONS

A multiproxy investigation of the sediment sequence in proglacial Lake Muzelle allowed the reconstruction of past glacier fluctuations using both detrital input and organic matter content over the last 1700 yr. Six periods of glacial extension were identified in the watershed (AD 370–500, AD 1080–1100, AD 1230–1325, AD 1460–1500, AD 1615–1790, and AD 1820–1900), which agree with records from reference glaciers in the Alps. In addition, analysis of the sediment revealed 255 interbedded layers characterized by coarse-grained bases and fining-upward trends. Their characteristics and occurrence suggest that they were formed by high-energy turbidity currents transporting sediment during extreme precipitation events, which is also supported by comparison with historical floods during the last century.

Despite differences in climate forcing between glacial activity, which is classically driven by winter precipitation and summer temperatures, and flood occurrence, which is driven by extreme rainfall events, we found similar trends. This relationship is explained by the presence of fine sediment produced by glacial abrasion in the watershed. During periods of increased glacial extent, an increased presence of fine sediment is observed both in the continuous sedimentation and the flood layers within the lake. The flood deposits exhibit increased thicknesses with finer grain sizes compared with periods when the glacier had retreated. We interpret this fine sediment as having been transported by the glacial stream and heavy rainfall to the proglacial lake. The presence of the Muzelle glacier may have maintained favorable hydrologic conditions for flood deposits to occur. Moreover, the presence of fine sediment probably increased the watershed sensitivity to induce the production of flood deposits in the lake system. Comparison of the Muzelle flood record with other flood records from the French and Swiss Alps highlights the distinctive features of the reconstruction, which indicate the importance of accounting for environmental shifts in the vicinity of the lake, especially in the proglacial context. There is a need to take environmental changes such as glacial variations into account in order to interpret flood records in terms of frequency and intensity.

ACKNOWLEDGMENTS

L. Fouinat's PhD fellowship was supported by a grant from Ecrins National Park, Communauté des Communes de l'Oisans, Deux Alpes Loisirs, and the Association Nationale de la Recherche et de la Technologie. The authors wish to thank Ecrins National Park for their permission to sample and assistance during the fieldwork. The authors are grateful to C. Vincent (LGGE laboratory UMR5183), who provided data on the St. Sorlin glacier, and L. Glur from the Swiss Federal Institute of Aquatic Science and Technology (Eawag), who provided data on the Trüebsee proglacial lake. All ^{14}C ages referred to as "SacA" were measured in the CEA Institute at Saclay (French Atomic Energy Commission). Thanks are extended to the CNRS-INSU ARTEMIS national radiocarbon AMS measurement program at LMC14 and Poznan Radiocarbon Laboratory for their constant help in the management of the ^{14}C samples and results. The authors thank the LSM for the gamma spectrometry measurements and Nicolas Thouveny for providing access to facilities at the CEREGE paleomagnetic laboratory (Aix-Marseille Université). Finally, we are grateful to Russell Drysdale for his comments and for correcting the English of this manuscript.

REFERENCES

Alexandrescu, M., Courtillot, V., Le Mouël, J., 1997. High-resolution secular variation of the geomagnetic field in western Europe over the last 4 centuries: comparison and integration of historical data from Paris and London. *Journal of Geophysical Research: Solid Earth* 102, 20245–20258.

Alley, R.B., Lawson, D.E., Larson, G.J., Evenson, E.B., Baker, G.S., 2003. Stabilizing feedbacks in glacier-bed erosion. *Nature* 424, 758–760.

Amann, B., Szidat, S., Grosjean, M., 2015. A millennial-long record of warm season precipitation and flood frequency for the northwestern Alps inferred from varved lake sediments: implications for the future. *Quaternary Science Reviews* 115, 89–100.

Appleby, P.G., Richardson, N., Nolan, P.J., 1991. ^{241}Am dating of lake sediments. In: Smith, J.P., Appleby, P.G., Battarbee, R.W., Dearing, J.A., Flower, R., Haworth, E.Y., Oldfield, F., O'Sullivan, P.E. (Eds.), *Environmental History and Palaeolimnology. Developments in Hydrobiology* Vol. 67. Springer, Dordrecht, the Netherlands, pp. 35–42.

Arnaud, F., Lignier, V., Revel, M., Desmet, M., Beck, C., Pourchet, M., Charlet, F., Trentesaux, A., Tribovillard, N., 2002. Flood and earthquake disturbance of ^{210}Pb geochronology (Lake Anterne, NW Alps). *Terra Nova* 14, 225–232.

Bajard, M., Sabatier, P., David, F., Develle, A.-L., Reyss, J.-L., Fanget, B., Malet, E., *et al.*, 2016. Erosion record in Lake La Thuile sediments (Prealps, France): evidence of montane landscape dynamics throughout the Holocene. *Holocene* 26, 350–364.

https://doi.org/10.1017/qua.2017.18 Published online by Cambridge University Press

Bakke, J., Dahl, S.O., Paasche, Ø., Riis Simonsen, J., Kvisvik, B., Bakke, K., Nesje, A., 2010. A complete record of Holocene glacier variability at Austre Okstindbreen, northern Norway: an integrated approach. *Quaternary Science Reviews* 29, 1246–1262.

Balsam, W.L., Deaton, B.C., Damuth, J.E., 1998. The effects of water content on diffuse reflectance spectrophotometry studies of deep-sea sediment cores. *Marine Geology* 149, 177–189.

Beniston, M., 2007. Linking extreme climate events and economic impacts: examples from the Swiss Alps. *Energy Policy* 35, 5384–5392.

Blaauw, M., 2010. Methods and code for "classical" age-modelling of radiocarbon sequences. *Quaternary Geochronology* 5, 512–518.

Bøe, A.-G., Dahl, S.O., Lie, Ø., Nesje, A., 2006. Holocene river floods in the upper Glomma catchment, southern Norway: a high-resolution multiproxy record from lacustrine sediments. *Holocene* 16, 445–455.

Bogen, J., 1996. Erosion rates and sediment yields of glaciers. *Annals of Glaciology* 22, 48–52.

Boldt, B.R., Kaufman, D.S., McKay, N.P., Briner, J.P., 2015. Holocene summer temperature reconstruction from sedimentary chlorophyll content, with treatment of age uncertainties, Kurupa Lake, Arctic Alaska. *Holocene* 25, 641–650.

Büntgen, U., Tegel, W., Nicolussi, K., McCormick, M., Frank, D., Trouet, V., Kaplan, J.O., *et al*., 2011. 2500 Years of European climate variability and human susceptibility. *Science* 331, 578–582.

Bussmann, F., Anselmetti, F.S., 2010. Rossberg landslide history and flood chronology as recorded in Lake Lauerz sediments (Central Switzerland). *Swiss Journal of Geosciences* 103, 43–59.

Casty, C., Wanner, H., Luterbacher, J., Esper, J., Böhm, R., 2005. Temperature and precipitation variability in the European Alps since 1500. *International Journal of Climatology* 25, 1855–1880.

Dahl, S.O., Bakke, J., Lie, Ø., Nesje, A., 2003. Reconstruction of former glacier equilibrium-line altitudes based on proglacial sites: an evaluation of approaches and selection of sites. *Quaternary Science Reviews* 22, 275–287.

Dahl, S.O., Nesje, A., 1994. Holocene glacier fluctuations at Hardangerjøkulen, central-southern Norway: a high-resolution composite chronology from lacustrine and terrestrial deposits. *Holocene* 4, 269–277.

Dahlke, H.E., Lyon, S.W., Stedinger, J.R., Rosqvist, G., Jansson, P., 2012. Contrasting trends in floods for two sub-arctic catchments in northern Sweden – does glacier presence matter? *Hydrology and Earth System Sciences* 16, 2123–2141.

Debret, M., Desmet, M., Balsam, W., Copard, Y., Francus, P., Laj, C., 2006. Spectrophotometer analysis of Holocene sediments from an anoxic fjord: Saanich Inlet, British Columbia, Canada. *Marine Geology* 229, 15–28.

Debret, M., Sebag, D., Desmet, M., Balsam, W., Copard, Y., Mourier, B., Susperrigui, A.-S., *et al*., 2011. Spectrocolorimetric interpretation of sedimentary dynamics: the new "Q7/4 diagram. *Earth-Science Reviews* 109, 1–19.

Desloges, J.R., 1994. Varve deposition and the sediment yield record at three small lakes of the southern Canadian Cordillera. *Arctic and Alpine Research* 26, 130–140.

Diolaiuti, G.A., Maragno, D., D'Agata, C., Smiraglia, C., Bocchiola, D., 2011. Glacier retreat and climate change: documenting the last 50 years of Alpine glacier history from area and geometry changes of Dosde Piazzi glaciers (Lombardy Alps, Italy). *Progress in Physical Geography* 35, 161–182.

Dyurgerov, M.B., Meier, M.F., 2000. Twentieth century climate change: evidence from small glaciers. *Proceedings of the National Academy of Sciences of the United States of America* 97, 1406–1411.

Etienne, D., Jouffroy-Bapicot, I., 2014. Optimal counting limit for fungal spore abundance estimation using *Sporormiella* as a case study. *Vegetation History and Archaeobotany* 23, 743–749.

Etienne, D., Wilhelm, B., Sabatier, P., Reyss, J.-L., Arnaud, F., 2013. Influence of sample location and livestock numbers on *Sporormiella* concentrations and accumulation rates in surface sediments of Lake Allos, French Alps. *Journal of Paleolimnology* 49, 117–127.

Faegri, K., Kaland, P.E., Krzywinski, K., 1989. *Textbook of Pollen Analysis*. John Wiley and Sons, New York.

Gardent, M., 2014. Inventaire et retrait des glaciers dans les alpes françaises depuis la fin du Petit Age Glaciaire. PhD dissertation, Université de Grenoble, Grenoble, France.

Gardent, M., Rabatel, A., Dedieu, J.-P., Deline, P., 2014. Multi-temporal glacier inventory of the French Alps from the late 1960s to the late 2000s. *Global and Planetary Change* 120, 24–37.

Giguet-Covex, C., Arnaud, F., Enters, D., Poulenard, J., Millet, L., Francus, P., David, F., Rey, P.-J., Wilhelm, B., Delannoy, J.-J., 2012. Frequency and intensity of high-altitude floods over the last 3.5ka in northwestern French Alps (Lake Anterne). *Quaternary Research* 77, 12–22.

Gilbert, R., Shaw, J., 1981. Sedimentation in proglacial Sunwapta Lake, Alberta. *Canadian Journal of Earth Sciences* 18, 81–93.

Gilli, A., Anselmetti, F.S., Glur, L., Wirth, S.B., 2013. Lake sediments as archives of recurrence rates and intensities of past flood events. In: Schneuwly-Bollschweiler, M., Stoffel, M., Rudolf-Miklau, F. (Eds.), *Dating Torrential Processes on Fans and Cones*. Springer, Dordrecht, the Netherlands, pp. 225–242.

Glur, L., Stalder, N.F., Wirth, S.B., Gilli, A., Anselmetti, F.S., 2014. Alpine lacustrine varved record reveals summer temperature as main control of glacier fluctuations over the past 2250 years. *Holocene* 25, 280–287.

Glur, L., Wirth, S.B., Büntgen, U., Gilli, A., Haug, G.H., Schär, C., Beer, J., Anselmetti, F.S., 2013. Frequent floods in the European Alps coincide with cooler periods of the past 2500 years. *Scientific Reports* 3, 2770. http://dx.doi.org/10.1038/srep02770.

Gobiet, A., Kotlarski, S., Beniston, M., Heinrich, G., Rajczak, J., Stoffel, M., 2014. 21st century climate change in the European Alps—a review. *Science of the Total Environment* 493, 1138–1151.

Goldberg, E.D., 1963. Geochronology with 210Pb. *Radioactive dating* 121.

Hallet, B., Hunter, L., Bogen, J., 1996. Rates of erosion and sediment evacuation by glaciers: a review of field data and their implications. *Global and Planetary Change* 12, 213–235.

Heiri, O., Lotter, A.F., Lemcke, G., 2001. Loss on ignition as a method for estimating organic and carbonate content in sediments: reproducibility and comparability of results. *Journal of Paleolimnology* 25, 101–110.

Hicks, D.M., McSaveney, M.J., Chinn, T.J.H., 1990. Sedimentation in proglacial Ivory Lake, Southern Alps, New Zealand. *Arctic and Alpine Research* 22, 26–42.

Hodder, K.R., Gilbert, R., Desloges, J.R., 2007. Glaciolacustrine varved sediment as an alpine hydroclimatic proxy. *Journal of Paleolimnology* 38, 365–394.

Holzhauser, H., Magny, M.J., Zumbühl, H.J., 2005. Glacier and lake-level variations in west-central Europe over the last 3500 years. *Holocene* 15, 789–801.

Jenny, J.-P., Wilhelm, B., Arnaud, F., Sabatier, P., Giguet Covex, C., Mélo, A., Fanget, B., Malet, E., Ployon, E., Perga, M.E.,

2014. A 4D sedimentological approach to reconstructing the flood frequency and intensity of the Rhône River (Lake Bourget, NW European Alps). *Journal of Paleolimnology* 51, 469–483.

Karlén, W., 1976. Lacustrine sediments and tree-limit variations as indicators of Holocene climatic fluctuations in Lappland, northern Sweden. *Geografiska Annaler: Series A, Physical Geography* 58, 1–34.

Koppes, M.N., Hallet, B., 2002. Influence of rapid glacial retreat on the rate of erosion by tidewater glaciers. *Geology* 30, 47–50.

Lanza, R., Meloni, A., Tema, E., 2005. Historical measurements of the Earth's magnetic field compared with remanence directions from lava flows in Italy over the last four centuries. *Physics of the Earth and Planetary Interiors* 148, 97–107.

Leemann, A., Niessen, F., 1994. Holocene glacial activity and climatic variations in the Swiss Alps: reconstructing a continuous record from proglacial lake sediments. *Holocene* 4, 259–268.

Leonard, E.M., 1997. The relationship between glacial activity and sediment production: evidence from a 4450-year varve record of neoglacial sedimentation in Hector Lake, Alberta, Canada. *Journal of Paleolimnology* 17, 319–330.

Le Roy, M., Nicolussi, K., Deline, P., Astrade, L., Edouard, J.-L., Miramont, C., Arnaud, F., 2015. Calendar-dated glacier variations in the western European Alps during the Neoglacial: the Mer de Glace record, Mont Blanc massif. *Quaternary Science Reviews* 108, 1–22.

Lurcock, P.C., Wilson, G.S., 2012. PuffinPlot: a versatile, user-friendly program for paleomagnetic analysis. *Geochemistry, Geophysics, Geosystems* 13, Q06Z45. http://dx.doi.org/10.1029/2012GC004098.

Menounos, B., Clague, J.J., 2008. Reconstructing hydro-climatic events and glacier fluctuations over the past millennium from annually laminated sediments of Cheakamus Lake, southern Coast Mountains, British Columbia, Canada. *Quaternary Science Reviews* 27, 701–713.

Micheletti, N., Lane, S.N., 2016. Water yield and sediment export in small, partially glaciated Alpine watersheds in a warming climate. *Water Resources Research* 52, 4924–4943.

Navratil, O., Evrard, O., Esteves, M., Legout, C., Ayrault, S., Némery, J., Mate-Marin, A., *et al*., 2012. Temporal variability of suspended sediment sources in an alpine catchment combining river/rainfall monitoring and sediment fingerprinting. *Earth Surface Processes and Landforms* 37, 828–846.

Nesje, A., Kvamme, M., Rye, N., Løvlie, R., 1991. Holocene glacial and climate history of the Jostedalsbreen region, western Norway; evidence from lake sediments and terrestrial deposits. *Quaternary Science Reviews* 10, 87–114.

Nesje, A., Matthews, J.A., Dahl, O., Berrisford, M.S., Andersson, C., 2001. Holocene glacier fluctuations of Flatebreen and winter-precipitation changes in the Jostedalsbreen region, western Norway, based on glaciolacustrine sediment records. *Holocene* 11, 267–280.

Nussbaumer, S.U., Steinhilber, F., Trachsel, M., Breitenmoser, P., Beer, J., Blass, A., Grosjean, M., *et al*., 2011. Alpine climate during the Holocene: a comparison between records of glaciers, lake sediments and solar activity. *Journal of Quaternary Science* 26, 703–713.

Oerlemans, J., 2005. Extracting a climate signal from 169 glacier records. *Science* 308, 675–677.

Oerlemans, J., Reichert, B., 2000. Relating glacier mass balance to meteorological data by using a seasonal sensitivity characteristic. *Journal of Glaciology* 46, 1–6.

Ohlendorf, C., Niessen, F., Weissert, H., 1997. Glacial varve thickness and 127 years of instrumental climate data: a comparison. *Climatic Change* 36, 391–411.

Owen, L.A., Derbyshire, E., Scott, C.H., 2003. Contemporary sediment production and transfer in high-altitude glaciers. *Sedimentary Geology* 155, 13–36.

Passega, R., 1964. Grain size representation by CM patterns as a geological tool. *Journal of Sedimentary Research* 34, 830–847.

R Development Core Team. 2011. The R Reference Manual. Network Theory, Bristol, UK.

Reimer, P.J., Bard, E., Bayliss, A., Beck, J.W., Blackwell, P.G., Ramsey, C.B., Buck, C.E., Cheng, H., Edwards, R.L., Friedrich, M., 2013. IntCal13 and Marine13 radiocarbon age calibration curves 0–50,000 years cal BP. *Radiocarbon* 55, 1869–1887.

Rein, B., Lückge, A., Reinhardt, L., Sirocko, F., Wolf, A., Dullo, W.-C., 2005. El Niño variability off Peru during the last 20,000 years. *Paleoceanography* 20, PA4003. http://dx.doi.org/10.1029/2004PA001099.

Rein, B., Sirocko, F., 2002. In-situ reflectance spectroscopy – analysing techniques for high-resolution pigment logging in sediment cores. *International Journal of Earth Sciences* 91, 950–954.

Reyss, J.-L., Schmidt, S., Legeleux, F., Bonté, P., 1995. Large, low background well-type detectors for measurements of environmental radioactivity. *Nuclear Instruments and Methods in Physics Research Section A: Accelerators, Spectrometers, Detectors and Associated Equipment* 357, 391–397.

Rickenmann, D., D'Agostino, V., Fontana, G.D., Lenzi, M., Marchi, L., 1998. New results from sediment transport measurements in two Alpine torrents. In: Kovar, K., Tappeiner, U., Peters, N.E., Craig, R.G. (Eds.), Hydrology, Water Resources and Ecology in Headwaters (Proceedings of the HeadWater '98 Conference held at Meran/Merano, Italy, from 20 to 23 April 1998). IAHS Publication No. 248. International Association of Hydrological Sciences, Wallingford, Oxfordshire, UK, pp. 283–290.

Riihimaki, C.A., MacGregor, K.R., Anderson, R.S., Anderson, S.P., Loso, M.G., 2005. Sediment evacuation and glacial erosion rates at a small alpine glacier. *Journal of Geophysical Research: Earth Surface* 110, F03003. http://dx.doi.org/10.1029/2004JF000189.

Sabatier, P., Dezileau, L., Briqueu, L., Colin, C., Siani, G., 2010. Clay minerals and geochemistry record from northwest Mediterranean coastal lagoon sequence: implications for paleostorm reconstruction. *Sedimentary Geology* 228, 205–217.

Schiefer, E., Gilbert, R., Hassan, M.A., 2011. A lake sediment-based proxy of floods in the Rocky Mountain Front Ranges, Canada. *Journal of Paleolimnology* 45, 137–149.

Simonneau, A., Chapron, E., Garçon, M., Winiarski, T., Graz, Y., Chauvel, C., Debret, M., Motelica-Heino, M., Desmet, M., Di Giovanni, C., 2014. Tracking Holocene glacial and high-altitude alpine environments fluctuations from minerogenic and organic markers in proglacial lake sediments (Lake Blanc Huez, Western French Alps). *Quaternary Science Reviews* 89, 27–43.

Steiner, D., Pauling, A., Nussbaumer, S.U., Nesje, A., Luterbacher, J., Wanner, H., Zumbühl, H.J., 2008. Sensitivity of European glaciers to precipitation and temperature – two case studies. *Climatic Change* 90, 413–441.

Stockmarr, J., 1971. Tablets with spores used in absolute pollen analysis. *Pollen et spores* 13, 615–621.

Støren, E.N., Paasche, Ø., 2014. Scandinavian floods: from past observations to future trends. *Global and Planetary Change* 113, 34–43.

https://doi.org/10.1017/qua.2017.18 Published online by Cambridge University Press

Swierczynski, T., Lauterbach, S., Dulski, P., Delgado, J., Merz, B., Brauer, A., 2013. Mid- to late Holocene flood frequency changes in the northeastern Alps as recorded in varved sediments of Lake Mondsee (Upper Austria). *Quaternary Science Reviews* 80, 78–90.

Trachsel, M., Kvisvik, B.C., Nielsen, P.R., Bakke, J., Nesje, A., 2013. Inferring organic content of sediments by scanning reflectance spectroscopy (380–730 nm): applying a novel methodology in a case study from proglacial lakes in Norway. *Journal of Paleolimnology* 50, 583–592.

van der Bilt, W.G.M., Bakke, J., Vasskog, K., D'Andrea, W.J., Bradley, R.S., Ólafsdóttir, S., 2015. Reconstruction of glacier variability from lake sediments reveals dynamic Holocene climate in Svalbard. *Quaternary Science Reviews* 126, 201–218.

van Geel, B., Aptroot, A., 2006. Fossil ascomycetes in Quaternary deposits. *Nova Hedwigia* 82, 313–329.

van Geel, B., Buurman, J., Brinkkemper, O., Schelvis, J., Aptroot, A., van Reenen, G., Hakbijl, T., 2003. Environmental reconstruction of a Roman Period settlement site in Uitgeest (The Netherlands), with special reference to coprophilous fungi. *Journal of Archaeological Science* 30, 873–883.

Vincent, C., 2002. Influence of climate change over the 20th century on four French glacier mass balances. *Journal of Geophysical Research: Atmospheres* 107, 4375. http://dx.doi.org/10.1029/2001JD000832.

Vincent, C., Le Meur, E., Six, D., Funk, M., 2005. Solving the paradox of the end of the Little Ice Age in the Alps. *Geophysical Research Letters* 32, L09706. http://dx.doi.org/10.1029/2005GL022552.

Weirich, F.H., 1985. Sediment budget for a high energy glacial lake. *Geografiska Annaler: Series A, Physical Geography* 67, 83–99.

Wilhelm, B., Arnaud, F., Sabatier, P., Crouzet, C., Brisset, E., Chaumillon, E., Disnar, J.-R., *et al*., 2012. 1400 years of extreme precipitation patterns over the Mediterranean French Alps and possible forcing mechanisms. *Quaternary Research* 78, 1–12.

Wilhelm, B., Arnaud, F., Sabatier, P., Magand, O., Chapron, E., Courp, T., Tachikawa, K., *et al*., 2013. Palaeoflood activity and climate change over the last 1400 years recorded by lake sediments in the north-west European Alps. *Journal of Quaternary Science* 28, 189–199.

Wilhelm, B., Nomade, J., Crouzet, C., Litty, C., Sabatier, P., Belle, S., Rolland, Y., Revel, M., Courboulex, F., Arnaud, F., 2016. Quantified sensitivity of small lake sediments to record historic earthquakes: implications for paleoseismology. *Journal of Geophysical Research: Earth Surface* 121, 2–16.

Wilhelm, B., Sabatier, P., Arnaud, F., 2015. Is a regional flood signal reproducible from lake sediments? *Sedimentology* 62, 1103–1117.

Wirth, S.B., Glur, L., Gilli, A., Anselmetti, F.S., 2013. Holocene flood frequency across the Central Alps – solar forcing and evidence for variations in North Atlantic atmospheric circulation. *Quaternary Science Reviews* 80, 112–128.

Wolfe, A.P., Vinebrooke, R.D., Michelutti, N., Rivard, B., Das, B., 2006. Experimental calibration of lake-sediment spectral reflectance to chlorophyll a concentrations: methodology and paleolimnological validation. *Journal of Paleolimnology* 36, 91–100.